Linear azimuthons in circular fiber arrays and optical angular momentum of discrete optical vortices

Article *in* Physical Review A · December 2009

DOI: 10.1103/PhysRevA.80.063821

CITATIONS
29

READS
128

1 author:

Constantine N Alexeyev
Crimean Federal University
123 PUBLICATIONS **1,030** CITATIONS

SEE PROFILE

Linear azimuthons in circular fiber arrays and optical angular momentum of discrete optical vortices

C. N. Alexeyev,* A. V. Volyar, and M. A. Yavorsky
Taurida National V.I. Vernadsky University, Vernadsky Prospekt 4, Simferopol 95007, Crimea, Ukraine
(Received 2 August 2009; published 8 December 2009)

We study the field generated in the outer space by the superposition of modes of a regular circular monomode fiber array. It is shown that a supermode of the fiber array generates a discrete optical vortex; the formula for the topological charge of the vortex is obtained depending on the order of the supermode and the number of fibers in the array. The orbital angular momentum carried by an arbitrary superposition of supermodes is shown to equal the weighted sum of partial angular momenta of supermodes. It is shown that for certain combinations of supermodes the angular momentum comprises along with its intrinsic part also the extrinsic constituent. For such combinations precession of the angular momentum about the propagation axis is demonstrated. It is demonstrated that by combining supermodes one can generate in the array stable regularly rotating linear azimuthons. By creating a phased excitation of certain groups of fibers in the array one can control the global soliton-like motion of the excited domain.

DOI: 10.1103/PhysRevA.80.063821 PACS number(s): 42.25.Bs, 42.81.Qb, 42.50.Tx

I. INTRODUCTION

Vortex phenomena are wide spread in nature, ranging from microscopic to macroscopic scales. Until quite recently, the presence of any vortex phenomena has been implicitly associated by physicists as a manifestation of some nonlinearity embedded into the system. In this connection, it proved surprising to find out from the early studies of the Bristol theory group [1,2] that vortices, being understood as phase dislocations of wave fronts, take place even in the systems described by linear equations, in particular, Maxwell's equations. Since then a lot of efforts have been made to form in modern optics the foundations of a special kind of paradigm, figuratively called by M. Berry a "vorticulture." Though the outlines of this novel branch of optics appeared as early as 1974, the notion of an optical vortex (OV) has been introduced somewhat later [3]. At present the OV is associated with the following features of the wave field: 1) the presence of intensity zero in the center of the vortex; 2) phase indefiniteness in this point; and 3) the presence of a screw dislocation of the wave front. For a scalar field Ψ the position of vortices is determined by the lines of zero intensity $\mathrm{Re}\,\Psi=\mathrm{Im}\,\Psi=0$. Near the vortex center, its behavior in the transverse plane is described as $\Psi\propto r^l\exp(il\varphi)$, where r,φ are the polar coordinates. A winding number l is the topological charge of the vortex, which determines the number of branches of the wave front helicoid [4]. Since at $r=0$ the phase is indefinite, this point is called a singularity point, namely, a phase singularity point. The concept of singularity points proved to be very fruitful and made it possible to generalize the theory beyond the limits of the scalar case describing singularities in vector fields [2,5]. In general, the branch of optics that studies various types of optical singularities has gotten the name of singular optics [6]. A special behavior of phase and amplitude near the vortex core result in a circular flow of energy in OVs. This property of OVs is closely connected with the ability of OVs to carry the angular momentum (AM) [7]. In combination with the property of zero intensity it makes a good ground for creation of optical traps on the basis of OVs [8]. Among other applications of OVs one should list using OVs for information transfer [9], in astrophysics [10], in microscopy [11] and micromachining [12].

In nonlinear media, OVs exist in the form of vortex solitons [13]. Being non-dissipative objects, vortex solitons seem to be promising information carriers [14]. Generally, in homogeneous nonlinear media OVs feature an azimuthal instability. One of the ways to achieve stabilization of vortex solitons is to use optically induced photonic lattices. Quite recently, a novel type of discrete (lattice) vortex solitons have been theoretically predicted [15] and experimentally observed [16] for square lattices. The analogy between discrete vortex (DV) solitons and azimuthons (or soliton clusters), was also noted in Ref. [17]. Also, in this paper. it has been provided a general relation between the order N of a discrete rotational symmetry of the system and the value of the maximal topological charge m of the DV, which can be created in it: $|m|\leq N/2$. Later this question of the so called vorticity cutoff has been addressed in a number of papers, in which it has been revealed the connection of this rule with basic symmetries of discrete systems [18,19]. It has also been studied the processes of DV's transfigurations upon passage through the boundary between space areas with different types of symmetry [20]. DV solitons can also be created in photonic crystal fibers [21] and in other types of photonic lattices [22]. DVs are often associated with soliton clusters, which feature interesting mobility properties rotating upon propagation [14]. In general, the question of soliton dynamics in optical lattices is still drawing a great amount of attention [23]. In this connection there arises a general question whether a soliton-like motion of localized energy in photonic lattices is inherent only to nonlinear beam propagation or there are a number of vortex-beam structures in a linear wave motion that have similar characteristics.

The other question is concerned with the AM of DVs. Their distinguishing feature is a step-like behavior of their

*Corresponding author; alexeyev@ccssu.crimea.ua

phase [24] along the contour encompassing the phase singularity, which is dictated by the presence of the induced lattice. The dependence of the phase Φ in a DV can be roughly described as $\Phi(\varphi) \approx \Sigma_i \Delta\Phi_i \theta(\varphi - \varphi_i)$, θ being the unit step, where the phase jumps $\Delta\Phi_i$ occur at angles φ_i, which is in a drastic contrast to the expression for the phase in conventional OVs: $\Phi(\varphi) = l\varphi$. While it is known that an ordinary OV carries orbital AM (OAM) of $l\hbar$ per photon [7], the influence of the phase profile on the value of specific OAM, in DVs in particular, has never been demonstrated in the literature. Meanwhile, it is interesting to study whether is it sufficient for a vortex to have a phase increment of $2\pi l$ to guarantee its AM. The question of AM of DVs has also been addressed in Refs. [18,19] where it has been highlighted the questions connected with AM conservation in systems with discrete types of symmetry and some general statements on that matter have been made. However, no particular example concerning calculation of AM of any DV has been provided, so that the question of the AM of a DV still remains under investigated.

To answer these questions in this paper we study the linear propagation of light in the simplest type of waveguide arrays—a circular array of single mode optical fibers, which modes form the set of DVs. The first aim of this paper is to study the OAM of the array's eigenmodes and demonstrate that, unlike "ordinary" OVs, the DVs can carry arbitrary low OAM per photon, depending on array parameters. Our emphasis here is to show conservation of the OAM of both the supermode and their linear superpositions. Our second objective is to demonstrate that linear superpositions of DVs can form the so-called linear azimuthons, in which a controllable circular soliton-like motion of energy is achieved. The last goal of the present paper is to study the OAM of linear azimuthons and determine conditions, at which their AM also comprises its extrinsic constituent.

II. LATTICE VORTICES IN CIRCULAR FIBER ARRAYS AND THEIR ANGULAR MOMENTUM

Evanescently coupled optical fiber arrays have evoked in the past years a great amount of attention due to their unique ability to mold the flow of light in ways that are impossible in homogeneous media [25]. In particular, fiber arrays allow light transfer control and diffraction management due to specific properties of discrete diffraction [26]. Along with immediate practical application, fiber arrays can be used for modeling processes not directly concern with optics [27]. One-dimensional fiber arrays form an important class of fiber arrays that was first theoretically addressed by A. Jones in 1965 [28]. Theoretical treatment of finite-element arrays is complicated by impossibility to solve analytically the dispersion equation for arbitrary number of array elements. In solid state physics, this difficulty is traditionally by-passed by using periodic Born-Karman boundary conditions [29]. In optics, this formal technique corresponds to linking the ends of the 1D array thus turning it into a circular fiber array.

A. Discrete vortex supermodes of circular fiber arrays

A circular fiber array is composed of N evanescently coupled fibers immersed into a medium with a universal refractive index and positioned at the vertices of a regular N-gone (see Fig. 1). Among main applications of circular arrays one should mention all optical switching and routing [30], discrete diffraction management [31]. Though this system has first been addressed thirty odd years ago by Snyder [32], it still remains of interest both in its linear [31–33] and nonlinear aspects [34,35]. Recently, circular fiber arrays have been proposed for generation of cylindrical vector beams [36]. Besides, circular array geometry is present in many types of photonic crystal fibers [21,37], which calls for further investigation of such arrays. In addition, a discrete character of diffraction in one-dimensional arrays leads to a number of interesting effects, such as a discrete Talbot effect and others [38].

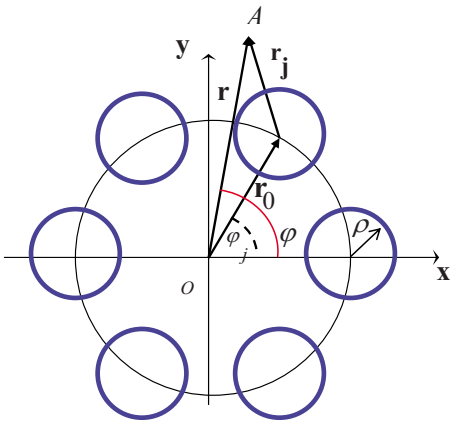

FIG. 1. (Color online) The model of a regular circular array of identical fibers. Effective radii of fundamental Gaussian-like modes are indicated with blue circles.

As is well established, propagation of light in a circular fiber array is governed by the set of coupled-mode equations (see, for example, Ref. [30]):

$$i\frac{da_n}{dz} = \tilde{\beta} a_n + \frac{J}{2}(a_{n+1} + a_{n-1}), \tag{1}$$

where $a_i(z)$ is the amplitude of the i-th fiber mode, $\tilde{\beta}$ is the scalar propagation constant of fundamental modes supported by individual (isolated) fibers of the array, J is the coupling constant. Circular form of the array is accounted in periodic boundary conditions: $a_{i+N} = a_i$. As is known, Eq. (1) is readily solved through a discrete (lattice) Fourier transform (see, for example, Ref. [26]). Its solution yields for the eigenmodes X_m the following linear combinations of fundamental modes q_k of k-th fiber:

$$X_m = \frac{1}{\sqrt{N}} \sum_{k=0}^{N-1} \exp\left(\frac{2i\pi m}{N} k\right) q_k, \tag{2}$$

where $|m| = 0, 1, \ldots, N-1$. Combinations Eq. (2) are conventionally called the supermodes of a circular array. The propagation constant of the m-th supermode equals to:

$$\beta_m = \tilde{\beta} + J\cos\left(\frac{2\pi m}{N}\right). \tag{3}$$

Any initial excitation of the array decomposes in its supermodes Eq. (2) that propagate with phase velocities determined by Eq. (3). This process of discrete diffraction is summarized in the following expression describing the evolution of an initial excitation $\vec{Y}=(Y_0, Y_1, \ldots, Y_{N-1})$ created at the input ($z=0$) end of the fiber array:

$$\Psi(z) = \sum_{k,l,n=0}^{N-1} Y_k q_n \exp\{2i\pi l(n-k)/N\}\exp(i\beta_l z), \tag{4}$$

where Ψ is the superposition of individual fiber's fields, Y_k is the input amplitude of the mode of a k-th fiber.

Until quite recently, the main importance of Eq. (4) was connected with its ability to predict the values of z-dependent amplitudes $Y_n(z)=\Sigma_{k,l}Y_k \exp\{2i\pi l(n-k)/N\}\exp(i\beta_l z)$, which describe just one-site distribution of energy. However, in past few years the focus of research has been somewhat shifted to the points beyond the fiber array. New types of questions became characteristics for such studies, in particular, what kind of field is being formed outside the array's fibers [36]. This proves to have much in common with the studies of beam arrays, where the fact that combination of beams may possess the property none of the beams ever had has been well established [39]. Following the ideas of Ref. [39], let us consider the structure of the field of the mode Eq. (2) in the transverse plane.

For simplicity we suppose that the circular array is composed of weakly guiding step-index fibers. Then the electric field of an individual j-th fiber Ψ_j can be represented in the Gaussian approximation as [32]:

$$\Psi_j^{(l)} = E\exp\left(-\frac{r_j^2}{2\rho^2}\right), \tag{5}$$

where $\varphi_j=\frac{2\pi}{N}j$, j is integer and $l=0, \pm 1, \ldots, \pm(N-1)$, so that $X_l=\Sigma_{j=0}^{N-1}\Psi_j^{(l)}\exp(il\varphi_j)$, ρ is the effective radius of the fundamental mode defined for step-index fibers as: $\rho=\frac{\rho_0}{\sqrt{2\ln V}}$, where ρ_0 is the core's radius and V is the waveguide parameter. Here, r_j is measured from the center of the j-th core (see Fig. 1). Since $r_j^2=r^2+r_0^2-2rr_0\cos(\varphi-\varphi_j)$, where r_0 is the radius of the array, the total field of the supermode can be written as:

$$X_l = E\exp\left(-\frac{r^2+r_0^2}{2\rho^2}\right)\sum_{j=0}^{N-1}\exp\left[\frac{rr_0}{\rho^2}\cos(\varphi-\varphi_j)+il\varphi_j\right]. \tag{6}$$

As follows from Eq. (2), the phase shift between adjacent sites for the m-th supermodes is $\frac{2\pi m}{N}$, so that the total phase increment for a contour encompassing the origin $r=0$ is $2\pi m$. This seems to be proving that the field Eq. (6) describes some OV of topological charge m. However, there is a subtlety to this otherwise transparent result. As has been mentioned [39], asymptotics of the field Eq. (6) at the origin $r=0$ give for the charge of the vortex a different value. Indeed, using a well-known decomposition [32]:

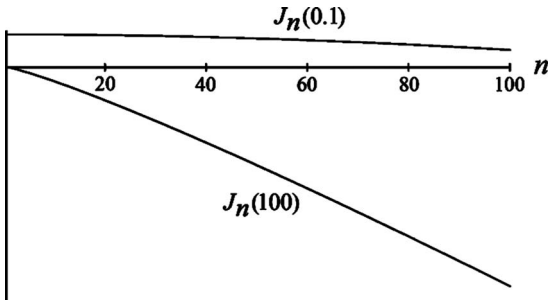

FIG. 2. Dependence of Bessel functions $I_n(z)$ in a semi log scale on their order for certain values of z: solid line $z=100$; dashed line $z=0.01$.

$$\exp(z\cos\alpha) = \sum_{k=-\infty}^{\infty} I_k(z)\exp(ik\alpha), \tag{7}$$

where I_k is the Bessel function, one readily obtains from Eq. (6):

$$X_l = \Gamma\sum_{j=0}^{N-1}\sum_{k=-\infty}^{\infty} I_k(z)\exp\{i[k\varphi+(l-k)\varphi_j]\}, \tag{8}$$

where $\Gamma=E\exp(-\frac{r^2+r_0^2}{2\rho^2})$, $z=\frac{rr_0}{\rho^2}$. Allowing for Ref. [39]:

$$\sum_{j=0}^{N-1}\exp(in\varphi_j) = N\delta_{n,mN}, \quad m=0, \pm 1, \ldots, \tag{9}$$

where δ_{ik} is Kronecker delta, one arrives at:

$$X_l = \Gamma N\sum_{m=-\infty}^{\infty} I_{mN+l}(z)\exp[i(mN+l)\varphi]. \tag{10}$$

Here, the supermode X_l is decomposed in OVs with different coefficients at a given r. It should be noted that analogous decomposition is obtained even in the case where the exact expressions for fundamental modes are used, so that the results obtained within the Gaussian approximation coincide with the predictions of exact theory. To assess the topological charge of the series Eq. (10) one has to recall that the charge of combination of OVs is determined by the vortex, whose coefficient is the largest [2–4]. Owing to this fact the charge of X_l depends on the number ν obtained as:

$$I_\nu(z) = \max_n I_n(z). \tag{11}$$

It is a well-known fact from the theory of Bessel functions that at any real z one has: $I_0(z)>I_n(z)$ at $n\neq 0$. This can be easily proved using the integral representation of Bessel functions. Numerical simulations illustrate this fact for small and large z (see Fig. 2). As is also evident from this picture, at $x>0$ $I_x(z)$ is a monotonously decreasing function of x, so the topological charge $\mathfrak{I}$ of the supermode can be calculated as:

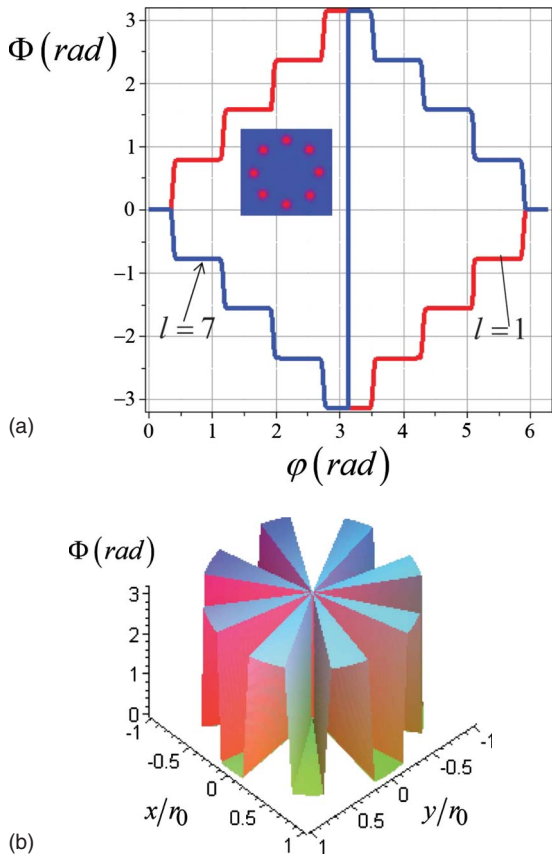

FIG. 3. (Color online) a) Phase distribution of discrete vortex supermodes X_1 and X_7 for an $N=8$ fiber array calculated at the distance r_0 from the origin. Due to the topological charge stroboscopic effect the mode X_7 in accordance with Eq. (13) features reverse phase increment that corresponds to a charge −1 D; b) Phase distribution of an l-fold edge dislocation supermode.

$$\mathfrak{I} = m_0 N + l, \tag{12}$$

where $m_0=\min|mN+l|$. Here, we have also allowed for the relation $I_\nu=\overset{m}{I}_{-\nu}$. In this way one can easily obtain for the topological charge of the l-th supermode:

$$\mathfrak{I} = \begin{cases} l, & \text{at } N > 2l \\ l - N, & \text{at } N < 2l \end{cases}. \tag{13}$$

For arrays of Gaussian beams in the limit $r\to 0$ this result has been obtained in Ref. [39]. It should be emphasized that this property of circular arrays is a particular example of a global rule for the charge of OVs in azimuthally modulated photonic lattices [17–20,40]. More involved situations concerning topological charge of DVs in discrete-symmetry media has recently been addressed in [41]. Numerical results confirm this conclusion [see Fig. 3(a)]. The phase distribution at some distance from the vortex core has a specific step-like form, characteristic to DVs [15–21] and solitons clusters [14], which enables us to identify the l-th supermode with the DV of charge $\mathfrak{I}$.

In the particular case $N=2l$ expression (10) has the following form:

$X_l=\Gamma N\Sigma_{m=-\infty}^{\infty} I_{l(2m+1)}(z)\exp[il(2m+1)\varphi]$
$=2\Gamma N\Sigma_{k=0}^{\infty} I_{l(2k+1)}(z)\cos[l(2k+1)\varphi]$. Each term in this sum describes an $l(2k+1)$-fold edge dislocation and no OV is formed. To classify the field X_l it is necessary to determine whether there exist such angles, at which all the terms in the structure of X_l simultaneously equal to zero. Obviously, the first term vanishes at $\varphi_n=\frac{2n+1}{l}\frac{\pi}{2}$. It is easily verified that other terms are also zero at $\varphi=\varphi_n$, so that the field of the mode X_l is zero at all angles φ_n and in this way describes an l-fold edge dislocation [see Fig. 3(b)]. So, it proves impossible to generate a supermode with topological charge more than $N/2$. Trying to exceed this limit results in changing the sign of the created OV. The reason of this topological charge "stroboscopic" effect is that the phase at a site is defined within 2π and a large phase increment between the sites can be interpreted by the system as a lesser and negative intersite phase difference. For example, at $N=3$ the phases at the sites for $l=2$ are 0, $\frac{4\pi}{3}$ and $\frac{8\pi}{3}$. By "subtracting" 2π from these phases the array turns this $l=2$ OV into $l=-1$ OV with a modified phase distribution: -2π, $-\frac{4\pi}{3}$, and $-\frac{2\pi}{3}$. Recently, a number of techniques for generation of OVs has been suggested where the vortex is generated by discrete phase-changing elements. The described change stroboscopic effect puts a natural limitation to the value of topological charge, which can be generated by a system consisting of N phase-changing elements and should be taken into consideration.

B. Angular momentum of discrete vortices

Following Berry [42], we define the AM density as:

$$\vec{m} = \vec{r} \times (\vec{D} \times \vec{B}), \tag{14}$$

where Minkovski's definition of the field's momentum is adopted. The density of energy w is given by:

$$w = \frac{1}{2}(\vec{E}\cdot\vec{D} + \vec{H}\cdot\vec{B}). \tag{15}$$

Since in weakly guiding fibers light propagates paraxially, one can use a modification of Berry's relation [42] for spinless fields:

$$\frac{M_z}{W} = \frac{1}{\omega}\frac{\langle\psi|\hat{l}_z|\psi\rangle}{\langle\psi|\psi\rangle}, \tag{16}$$

where $\vec{M}=\int\int_S\langle\vec{m}\rangle dS$ is the time-averaged AM linear density, $W=\int\int_S\langle w\rangle dS$ is the time-averaged linear energy density, S is the transverse cross-section. As usual, time-averaging of bilinear combination of monochromatic (with frequency ω) fields A, B is carried out as: $\langle AB\rangle=\frac{1}{2}\mathrm{Re}\, AB^*$. In Eq. (16) $\hat{l}_z=-i\frac{\partial}{\partial\varphi}$ is the operator of the OAM and the scalar product is defined as: $\langle a|b\rangle=\int\int_S a^*b dS$. We have excluded the spin AM by assuming linear polarization of the supermode.

Consider first the energy of the l-th supermode. After a little algebra using the integral representation of Bessel functions and the known integral [43]:

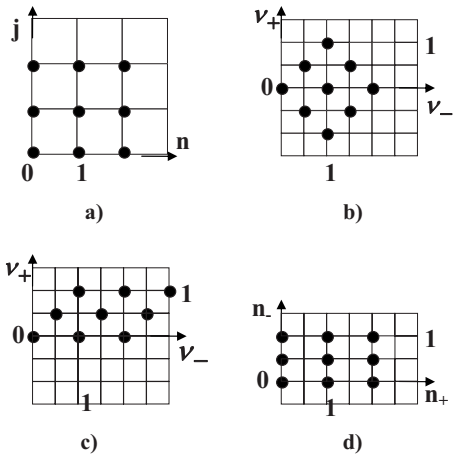

FIG. 4. To the change of variables Eq. (19): transformations of a square domain in variables (n,j) (a) into a square one in variables (n_+,n_-) (d) passes through the stages of a rhomb domain (b) and a parallelogram domain (c). The number of fibers is N=3. Note that the number of sites in the lattice does not change upon transformations and the step of the final summation over n_- is 1/2, whereas $|\Delta n_+|=1$.

$$\int_0^\infty e^{-at^2} t^{\nu+1} J_\nu(bt)dt = \frac{b^\nu}{(2a^2)^{\nu+1}} \exp\left(-\frac{b^2}{4a^2}\right), \tag{17}$$

one obtains for the denominator of Eq. (16):

$$\langle X_l | X_l \rangle \equiv \langle l|l\rangle = E^2 \pi \rho^2 \sum_{j,n=0}^{N-1} \exp\left[il(\varphi_n - \varphi_j) - \frac{r_0^2}{\rho^2} \sin^2 \frac{\varphi_n - \varphi_j}{2} \right]. \tag{18}$$

Since $W=\frac{1}{2}\varepsilon\varepsilon_0\langle\psi|\psi\rangle$ for paraxial beams, $W \propto \langle l|l\rangle$ and Eq. (18) determines the linear energy density of the supermode.

Here, it is convenient to pass to summation over new indices:

$$\nu_\pm = \frac{1}{2}(n \pm j). \tag{19}$$

There is a subtlety to this transition: simultaneously with it one has to change the summation area that is analogous to the change of integration domain. In our case the square domain in variables (n,j) turns into a rhomb in variables (ν_+,ν_-) (see Fig. 4), which makes it impossible to factorize immediately the sum over new variables. However, owning to the cyclic boundary conditions one can turn the rhomboid domain into a square one. In effect, the transition to variables Eq. (19) is carried out by a formal rule:

$$\sum_{n,j=0}^{N-1} f(n,j) = \sum_{n,j=0}^{N-1} \tilde{f}(\nu_+,\nu_-) = \sum_{n_+,n_-=0}^{N-1} \tilde{f}\left(n_+,\frac{1}{2}n_-\right), \tag{20}$$

where $n_\pm=0,1,\ldots N-1$. In this way Eq. (18) is reduced to:

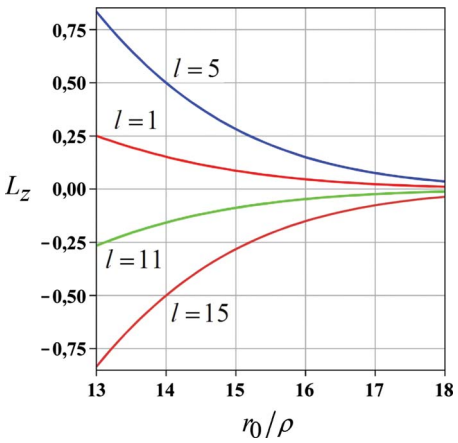

FIG. 5. (Color online) Orbital angular momentum (in AU) of a discrete vortex supermode vs array's radius; N=20.

$$\langle l|l\rangle = E^2 \pi \rho^2 N \sum_{n_-=0}^{N-1} \cos(l\varphi_-) \exp\left(-\frac{r_0^2}{\rho^2}\sin^2\frac{\varphi_-}{2}\right), \tag{21}$$

where $\varphi_\pm = \frac{2\pi n_\pm}{N}$ and we have allowed for realness of W. At $r_0 \gg \rho$ Eq. (21) can be approximately written as: $\langle l|l\rangle \approx \pi N E^2 \rho^2$, which corresponds to the total linear energy of N isolated fibers. It should be emphasized that disregarding the terms of higher order in $\exp(-\frac{r_0^2}{\rho^2})$ while deriving the power (energy) of an array is equivalent to the approximation of isolated fibers [32]. In this way Eq. (21) gives the corrections to this approximation.

In the same manner one can obtain the expression for $\langle l|\hat{l}_z|l\rangle$:

$$\langle l|\hat{l}_z|l\rangle = \frac{N}{2} E^2 \pi r_0^2 \sum_{n_-=0}^{N-1} \sin\varphi_- \sin(l\varphi_-) \exp\left(-\frac{r_0^2}{\rho^2}\sin^2\frac{\varphi_-}{2}\right). \tag{22}$$

As follows from this relation, at $r_0 \gg \rho$ the specific AM of the supermode tends to zero, so that the AM of a circular array, unlike its energy, depends on correlation between individual fibers and vanishes in its absence regardless of a constant topological charge inherent to a supermode. This conclusion is confirmed by numerical simulations (see Fig. 5). As is evident, the AM of the mode is z-independent and conserved as the mode propagates in the z-direction. This fact does not comply with the statement made in Ref. [19] that in the systems with discrete rotational symmetry the z-component of the OAM is not conserved. First of all, it should be stressed that in the Noether theorem it is implied the conservation of dynamical values in the time domain and nothing is said directly about their z-dependence. Some kind of conservation laws for the fluxes of corresponding dynamical values for propagating beams can be derived as consequences from this theorem and has little to do with time conservation. In particular, for paraxially propagating beams the "dynamics" of the total OAM in a cross-section is governed by the Eq. [42]:

$$\frac{d\langle L_z\rangle}{dz} = \langle\Psi|\frac{1}{2}\left[\frac{\partial}{\partial\varphi}, n^2\right]_-|\Psi\rangle, \tag{23}$$

where $[\ldots,\ldots]_-$ stands for commutator. From this relation it follows that conservation of OAM in the z-domain of a field can be ensured by a less strict condition than axial symmetry of refractive index $\frac{\partial n}{\partial\varphi}=0$: OAM in a cross-section is conserved whenever $\langle\Psi|\frac{\partial n}{\partial\varphi}|\Psi\rangle$ is zero. The simplest example is provided by the known linearly polarized modes of elliptical fibers: as can be easily shown, their OAM is zero in any cross-section despite the fact that rotational symmetry is violated [44]. In this way, even in systems with no continuous rotational symmetry the OAM in the cross-section can be z-independent. The same applies to the systems with discrete rotational symmetry: nothing definite can be said about the conservation of OAM in a cross-section unless the "power" of OAM sources $\langle\Psi|\frac{\partial n}{\partial\varphi}|\Psi\rangle$ is calculated. It turns out that though the OAM of the vortex supermode in circular fiber arrays is no longer well defined, nevertheless, it is conserved.

It has repeatedly been emphasized that AM is not necessarily associated with the OV (see, for example, Ref. [45] and references therein). However, it is still possible to provide yet one more argumentation why the phase increment along a closed contour cannot alone guarantee the presence of OAM of the field. For AM density of, say, y-polarized paraxial field using the approach suggested in Ref. [42] one can obtain a simple expression:

$$\langle m_z\rangle = \frac{\varepsilon\varepsilon_0}{2\omega}\mathrm{Re}\,\overset{*}{E}\hat{l}_z E. \tag{24}$$

If one represents the electric field as $E=Ae^{i\Phi}$, where A is the real amplitude and Φ is the phase, then from Eq. (24) it follows: $\langle m_z\rangle=\frac{\varepsilon\varepsilon_0}{2\omega}A^2\frac{\partial\Phi}{\partial\varphi}$, or

$$\langle m_z\rangle = \frac{1}{\omega}\frac{\partial\Phi}{\partial\varphi}\langle w\rangle. \tag{25}$$

This remarkably simple local relation explains why the OAM of a supermode can be made arbitrary low in the circular array. Indeed, in a DV the phase changes most rapidly just along the equidistant lines between the neighboring fibers. However, in those areas the energy density is exponentially low. In the like manner, the energy density is the largest near the cores, where the phase changes slowly.

C. Conservation laws in circular fiber arrays

It has long been established and is easily verified that the set Eq. (1) has the first integral $\Sigma_n|a_n|^2=\mathrm{const}$. This conservation law corresponds to energy conservation in the approximation of isolated fibers, given by the term with $n_-=0$ in Eq. (21). However, it is principally impossible to obtain the higher order corrections to this result that allow for interference effects between the fields of individual fibers since no information about the behavior of fields in the transverse plane is given in Eq. (1). By the same reason Eq. (1) does not give any hint on the z-evolution of the AM, even in the lowest-order approximation. To study the question of whether the AM conserves, one has to use from the very start the exact expressions for the superposition of supermodes:

$$\Psi(z) = \sum_l C_l X_l \exp(i\beta_l z). \tag{26}$$

The AM of this field is proportional to:

$$M_z \propto \langle\Psi|\hat{l}_z|\Psi\rangle = \sum_{l,l'}\overset{*}{C}_{l'}C_l\langle l'|\hat{l}_z|l\rangle\exp[i(\beta_l-\beta_{l'})z], \tag{27}$$

[see notation introduced in Eq. (18)]. Carrying out integration over transverse spatial variables one can reduce the average to:

$$\langle l'|\hat{l}_z|l\rangle \propto \sum_{j,n}\exp[i(l\varphi_n - l'\varphi_j)]G(\varphi_n-\varphi_j), \tag{28}$$

where the expression for G can be easily established from Eq. (22), where it enters the sum. The transition to variables Eq. (19) leads to:

$$\langle l'|\hat{l}_z|l\rangle \propto \sum_{n_-}\exp[i(l+l')\varphi_-]G(\varphi_-)\sum_{n_+}\exp[i(l-l')\varphi_+]. \tag{29}$$

The sum over n_+ of the geometric progression is zero whenever $l\neq l'$, so that $\langle l'|\hat{l}_z|l\rangle\propto\delta_{l,l'}$, which entails z-independence of the AM:

$$M_z \propto \sum_l |C_l|^2\langle l|\hat{l}_z|l\rangle, \quad \frac{dM_z}{dz}=0. \tag{30}$$

In this way, the AM of mode superposition equals to the weighted sum of partial AM and does not depend on the position of the cross-section it is measured in.

For the sake of completeness we provide the proof of energy conservation presented in the same technique. In the same manner, one can obtain for the energy of superposition of supermodes:

$$W \propto \langle\Psi|\Psi\rangle = \sum_{l,l'}\overset{*}{C}_{l'}C_l\langle l'|l\rangle\exp[i(\beta_l-\beta_{l'})z]. \tag{31}$$

Analogously to Eq. (28), one can obtain:

$$\langle l'|l\rangle \propto \sum_{j,n}\exp[i(l\varphi_n - l'\varphi_j)]F(\varphi_n-\varphi_j), \tag{32}$$

where $F(\varphi_n-\varphi_j)$ enters the sum in Eq. (18). The transition to $n_\pm$ variables leads to factorization of the sum in Eq. (32) and to separation of the same geometric progression factor $\Sigma_n\exp[i(l-l')n]$. Finally, $\langle l'|l\rangle$ turns out to be proportional to $\delta_{l,l'}$ that entails conservation of energy:

$$W \propto \sum_l |C_l|^2\langle l|l\rangle, \quad \frac{dW}{dz}=0. \tag{33}$$

As follows from Eq. (33), the energy of superposition of modes equals to the sum of partial energies carried by the constituent modes and is conserved.

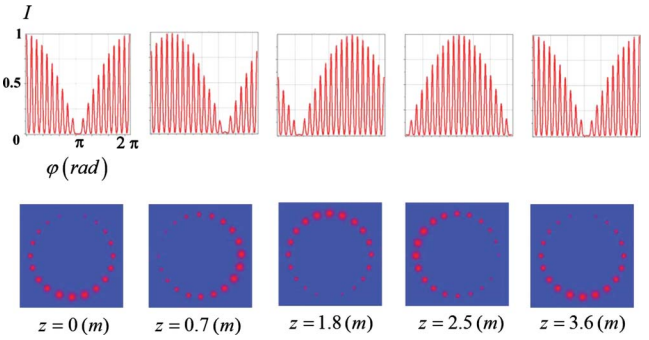

FIG. 6. (Color online) Evolution of intensity (I) distribution for equal-weight superposition of two supermodes X_1 and X_2 in an N=20 array; $J=2\pi$. The upper row shows intensity vs azimuthal angle.

III. LINEAR AZIMUTHONS IN CIRCULAR FIBER ARRAYS

Owing to unusual dispersion characteristics, discrete diffraction in fiber arrays exhibits properties never met in continuous systems [25]. These properties are efficiently used for one of the most important application of fiber arrays concerned with an optical switching and routing [30–36,46]. However, due to certain circumstances of a fundamental nature, in circular arrays it is impossible to switch all the energy from one fiber to other at arbitrary N [30]. To overcome this difficulty it has been suggested in a nonlinear case to control collective behavior of channels under excitation by managing their phase difference [35]. In this way the soliton-like all-optical switching is achieved in circular fiber arrays. In this section we demonstrate that such a technique is fruitful even in the linear case.

As is well established, excitation of a linear array with an equiphase perturbation leads to a discrete "diffusion" of an initial distribution of power. The simplest example of this process occurs when only one fiber of the array is excited [28]. To produce an ordered movement of the domain of lit fibers one has to correlate in the initial excitation the phases at the excited sites. For a circular array the simplest example of such correlated excitation is given by the excitation in the array the superposition of two supermodes with the same weights (see Fig. 6). In this case the field's distribution rotates as a whole. Excitation of other groups of supermodes may lead to different behavior of the input signal redistribution. So, adding four supermodes: $X_6+X_3-X_{-6}-X_{-3}$ in an array consisting of N=18 fibers one obtains no rotating intensity pattern, which, instead, features the presence of the discrete Talbot effect [38] (see Fig. 7). To achieve such control over the input signal one has to correlate excitation of a large number of fibers in the array. If one excites only a limited group of fibers, as suggested in Ref. [35], the result is less spectacular. The results of numerical simulations for various types of excitation profile are given in Fig. 8.

Such behavior of rotating patterns has direct analogy in one-dimensional infinite arrays. In this case, a mode of the array within a normalizing factor has the form: $X_k \propto \Sigma_n \exp(ikn+i\beta(k)z)q_n$, where we have included the propagation constant $\beta(k)=\tilde{\beta}+J\cos k$ into the structure of the

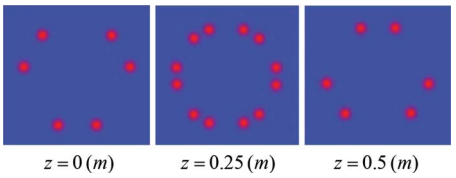

FIG. 7. (Color online) The discrete Talbot effect in circular arrays: initial pattern restoration under excitation of combination $X_6+X_3-X_{-6}-X_{-3}$ in array consisting of 18 fibers; J=6.28 (shown mirror-imaging at a half-period).

mode. It is possible to show that by combining, for example, two modes one obtains the pattern $X_k+X_{k'} \propto \Sigma_n A_n(k,k';z)q_n$ that features a homogeneous movement along the array. Indeed, as is easily verified, $|A_n(z)|^2=4\cos^2\{(k-k')n+z[\beta(k)-\beta(k')]\}$ so that initial excitation pattern displaces with constant velocity along the array as z increases. Such motion is also characteristic to discretely diffracted beams [25]. Being mapped onto circle by a technique suggested in Ref. [19], such linear motion produces rotational motion of a pattern with constant angular velocity, as shown in Fig. 6.

Most of the provided examples feature a distinct rotational movement of intensity distribution. These kinds of phenomena are well known in optics. It was reported for Laguerre-Gaussian (LG) beams by Kotlyar *et al.* [47]. More pronounced rotation was established for optical soliton clusters, which were identified with the so-called azimuthons [48]. Such rotating soliton complexes are also proved to exist in annular waveguides [49]. Recently, rotating intensity patterns in paraxial beams were recognized as linear azimuthons [50]. Circular fiber arrays provide especially good conditions for studying such types of phenomena. Rotating field patterns in them have an essential advantage in comparison with empty-space azimuthons: unlike the latter they maintain the constant rate of rotation and do not spread in the lateral direction. In addition, in contrast to nonlinear azimuthons they can be treated analytically to a much greater extent.

Even a superficial analysis of the given examples of linear azimuthons reveals their two main types. In some fields the pattern is symmetric about the origin $r=0$, whereas other fields feature asymmetry of intensity distribution (see Fig. 9).

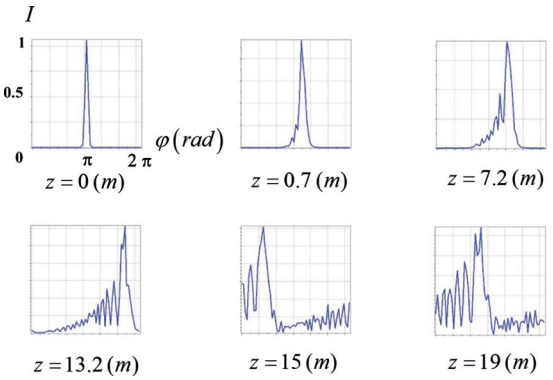

FIG. 8. (Color online) Spreading of a phased Gaussian profile in the circular array; $N=100$, $J=2\pi$. At the input z=0 only 5 fibers are excited. Intensity of initial excitation is described by a Gaussian envelope.

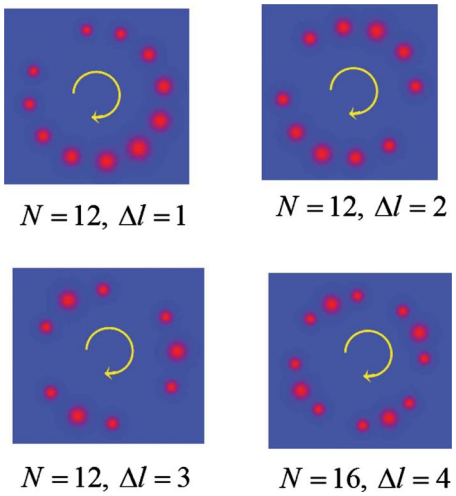

FIG. 9. (Color online) Intensity distribution patterns of linear azimuthons for superpositions of two supermodes with the difference Δl between mode numbers. Arrows indicate rotation direction.

To establish the conditions, at which the azimuthons in circular arrays are symmetric it is quite natural to study the position of a "center of gravity" of a beam. This useful concept is widely used in singular optics along with other mechanical analogies, and sheds light upon many aspects of electromagnetic field rotation [51]. For a field $|\Psi\rangle$ the coordinates $\bar{x}$, $\bar{y}$ of the center of gravity in the transverse cross-section can be defined as:

$$\bar{x} = \frac{\langle\Psi|x|\Psi\rangle}{\langle\Psi|\Psi\rangle}, \quad \bar{y} = \frac{\langle\Psi|y|\Psi\rangle}{\langle\Psi|\Psi\rangle}. \tag{34}$$

Consider a superposition of two supermodes with winding numbers l and l' (without the loss of generality one can assume $l' > l$):

$$\Psi(z) = C_l X_l \exp(i\beta_l z) + C_{l'} X_{l'} \exp(i\beta_{l'} z). \tag{35}$$

After some algebra one can obtain the following expression for the coordinates of the center of gravity of this superposition:

$$\bar{x} = R_c \cos[(\beta_{l'} - \beta_l)z + \arg \overset{*}{C_l} C_{l'}]\delta_{l',l+1},$$

$$\bar{y} = -R_c \sin[(\beta_{l'} - \beta_l)z + \arg \overset{*}{C_l} C_{l'}]\delta_{l',l+1}, \tag{36}$$

where

$$R_c = r_0 \frac{|C_l C_{l+1}| \sum_{n=0}^{N-1} \cos\frac{\varphi_n}{2} \cos\left[\left(l + \frac{1}{2}\right)\varphi_n\right] \exp\left(-\frac{r_0^2}{\rho^2}\sin^2\frac{\varphi_n}{2}\right)}{|C_l|^2 M_l + |C_{l+1}|^2 M_{l+1}} \tag{37}$$

and $M_l = \Sigma_{n=0}^{N-1} \cos l\varphi_n \exp(-\frac{r_0^2}{\rho^2}\sin^2\frac{\varphi_n}{2})$.

As follows from Eq. (36), the center of gravity displaces from the origin for any pair of modes with $|\Delta l| = 1$. In effect, the Kronecker delta in Eq. (36) expresses the existence of some kind of selection rule. In case the constituent modes do not comply with this selection rule, the center of gravity of the beam is in the origin. Otherwise it moves around a helical trajectory.

Fore more complicated combinations of modes the same reasoning is applicable. The contribution in the nominator of the right hand side of Eq. (34) would be given by any pair of constituent modes, which satisfy the selection rule $|\Delta l| = 1$.

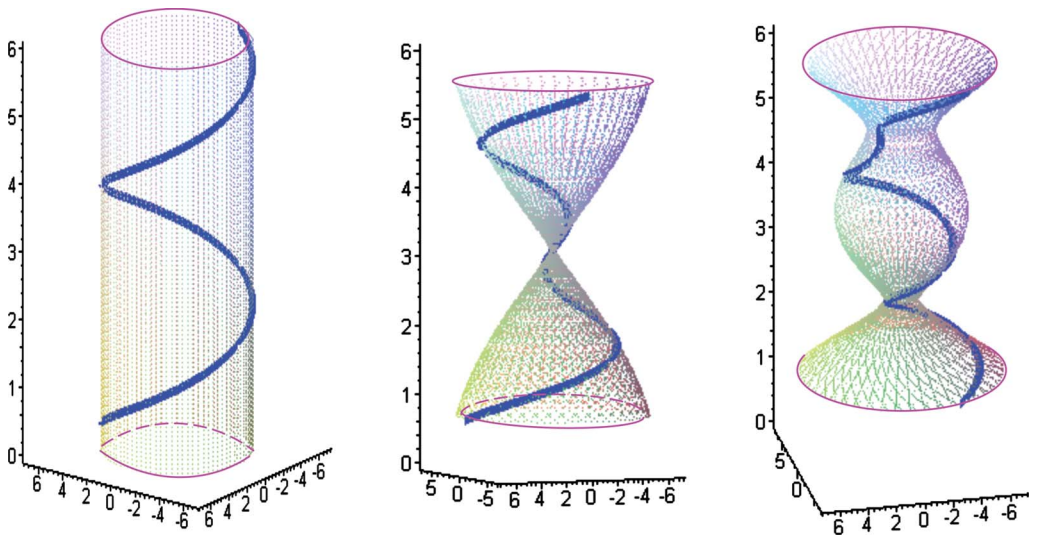

FIG. 10. (Color online) Trajectories of the center of gravity for superposition of several supermodes: (a) $-X_1+X_2$; (b) $-X_1+X_2+X_3$; (c) $-X_1+X_2+X_3+X_4$.

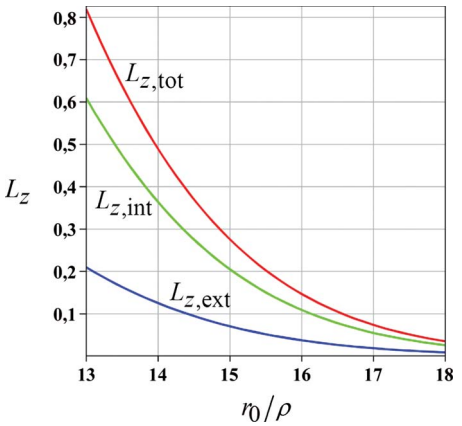

FIG. 11. (Color online) Intrinsic $L_{z,\mathrm{int}}$ and extrinsic $L_{z,\mathrm{ext}}$ parts of the total angular momentum $L_{z,\mathrm{tot}}$ in the cross-section vs array's radius for various supermodes; N=20.

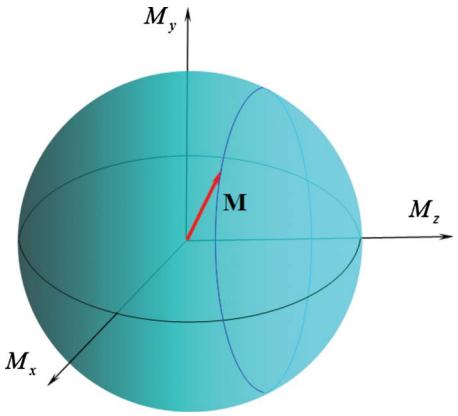

FIG. 12. (Color online) 12 Precession of the angular momentum in the cross-section for a combination of two supermodes.

The denominator, which is basically the energy of the field, will be the sum of energies. For a set of three supermodes with $l=1,2,3$ and equal weights, for example, the behavior of the center of gravity is given by:

$$\bar{x} = R_1 \cos[(\beta_2 - \beta_1)z] + R_2 \cos[(\beta_3 - \beta_2)z],$$

$$\bar{y} = -R_1 \sin[(\beta_2 - \beta_1)z] - R_2 \cos[(\beta_3 - \beta_2)z], \qquad (38)$$

where $R_1 = \frac{r_0}{M_\Sigma}\Sigma_{n=0}^{N-1}\cos\frac{\varphi_n}{2}\cos\frac{3\varphi_n}{2}\exp(-\frac{r_0^2}{\rho^2}\sin^2\frac{\varphi_n}{2})$,

$R_2 = \frac{r_0}{M_\Sigma}\Sigma_{n=0}^{N-1}\cos\frac{\varphi_n}{2}\cos\frac{5\varphi_n}{2}\exp(-\frac{r_0^2}{\rho^2}\sin^2\frac{\varphi_n}{2})$ and $M_\Sigma = M_1 + M_2 + M_3$. In this case $\bar{x}^2 + \bar{y}^2 = R_1^2 + R_2^2 + 2R_1R_2\cos[(\beta_3 - \beta_1)z]$, so that the radius of the center of gravity changes with z. The behavior of such linear azimuthon mimics some features of a breather soliton. The examples of trajectories of the center of gravity are given in Fig. 10.

IV. INTRINSIC AND EXTRINSIC ORBITAL ANGULAR MOMENTUM

Rotational motion of the center of gravity in linear azimuthons described in the previous Section gives rise to some interesting features in the behavior of the total AM. To understand their nature one has to recall that, as has been pointed out in Ref. [42], the linear AM density $\int\int_S \vec{m}dS$ generally proves to depend on the position of the origin of the frame, in which the AM is calculated. In this way under a shift of origin $\vec{r} \to \vec{r} + \vec{R}_c$ the linear AM density $\vec{M}$ changes as:

$$\vec{M} \to \vec{M} + \vec{R}_c \times \vec{P}, \qquad (39)$$

where $\vec{P} = \int\int_S \langle \vec{D} \times \vec{B} \rangle dS$ is the linear density of momentum by Minkosvki. As follows from Eq. (39), if $\vec{R}_c$ lies in the transverse cross-section, the AM $\vec{M}_o$ defined with respect to the origin O is connected with the AM $\vec{M}_c$ calculated in the frame centered in a point C through:

$$M_{oz} = M_{cz} + (\vec{R}_c \times \vec{P}_\perp)_z. \qquad (40)$$

Only in the case where $\vec{P}_\perp = \vec{0}$ the z-component of the AM does not depend on the position of the origin. This shift-independent AM is called intrinsic AM [52,53]. If this is not the case, intrinsic AM is the AM calculated in the system of center of gravity. If C is the center of gravity, the second term on the right of Eq. (40) gives the extrinsic part of the total AM.

To study the effect of center of gravity's motion on the AM of linear azimuthons it is convenient to express the components of electric and magnetic fields in terms of transverse electric field $\vec{E}_\perp$. This is most easily done in the paraxial case (approximation of weak guidance): for a monochromatic mode of frequency ω such expressions have the form:

$$E_z = \frac{i}{\beta}(\vec{\nabla}_\perp \bullet \vec{E}_\perp); \quad \vec{H}_\perp = \frac{\beta}{\omega\mu_0}\vec{n}_z \times \vec{E}_\perp;$$

$$H_z = -\frac{i}{\omega\mu_0}(\vec{\nabla}_\perp \times \vec{E}_\perp)_z, \qquad (41)$$

where $\vec{\nabla}_\perp = (\frac{\partial}{\partial x}, \frac{\partial}{\partial y})$ and $\vec{n}_z$ is the unit vector in the longitudinal direction. For an y-polarized electric field $\vec{E} = E\vec{n}_y$ time-averaged momentum density $\vec{p}_\perp$ assumes the form:

$$\langle \vec{p}_\perp \rangle = \frac{\varepsilon\varepsilon_0}{2\omega}\{\mathrm{Re}\, \overset{*}{E}(-i\vec{\nabla}_\perp)E + \beta|E|^2\vec{n}_z\}. \qquad (42)$$

Since also $\langle w \rangle = \frac{1}{2}\varepsilon\varepsilon_0|E|^2$ one obtains the expression that also has evident analogies in quantum mechanics [52]:

$$\frac{\langle \vec{p}_\perp \rangle}{\langle w \rangle} = \frac{1}{\omega}\frac{\langle \Psi | -i\vec{\nabla}_\perp | \Psi \rangle}{\langle \Psi | \Psi \rangle}. \qquad (43)$$

Now, we are in a position to calculate the transverse momentum.

It is straightforward to show that for a supermode $\vec{P}_\perp$ is zero. Analogously, consider transverse momentum for a superposition Eq. (35) of supermodes. In the same manner one can obtain for the ratio Eq. (43) the following result:

$$\frac{P_x}{W} = \frac{r_0}{\omega}Q_l \sin[(\beta_{l'} - \beta_l)z + \arg \overset{*}{C}_l C_{l'}]\delta_{l',l+1},$$

$$\frac{P_y}{W} = \frac{r_0}{\omega} Q_l \cos[(\beta_{l'} - \beta_l)z + \arg \overset{*}{C_l} C_{l'}]\delta_{l',l+1}, \tag{44}$$

where

$$Q_l = \frac{\frac{r_0}{\omega\rho^2}|C_l C_{l+1}| \sum_{n=0}^{N-1} \sin\frac{\varphi_n}{2} \sin\left[\left(l+\frac{1}{2}\right)\varphi_n\right] \exp\left(-\frac{r_0^2}{\rho^2}\sin^2\frac{\varphi_n}{2}\right)}{|C_l|^2 M_l + |C_{l+1}|^2 M_{l+1}}. \tag{45}$$

The Kronecker delta conveys the existence of the selection rule: the macroscopic transverse flow of energy takes place for supermodes with $|\Delta l| = 1$. This selection rule correlates with the one given by Eq. (36). This coincidence has a natural explanation: the change of energy distribution is always accompanied by the corresponding energy flow, which is proportional to momentum. From Eqs. (36) and (44) it follows the orthogonality of $\vec{R}_c = (\bar{x}, \bar{y})$ and $\vec{P}_\perp$:

$$\vec{R}_c \cdot \vec{P}_\perp = 0. \tag{46}$$

Since, as follows from Eq. (42), the longitudinal component of the total momentum remains constant: $\frac{P_z}{W} = \frac{kn_{co}}{\omega}$ the vector $\vec{P}$ undergoes a kind of precession and the total momentum is tangent to a helix.

Since the total AM of the supermode sum comprises both intrinsic and extrinsic constituents using Eq. (46) one can obtain from Eq. (40):

$$\frac{M_{oz}}{W} = R_c \frac{P_\perp}{W} + \frac{M_{cz}}{W}. \tag{47}$$

Here, the OAM of the superposition of two supermodes should be calculated in the frame centered in the point O using:

$$\frac{M_{oz}}{W} = \frac{r_0^2 \sum_{n=0}^{N-1} \sin\varphi_n \{|C_l|^2 \sin(l\varphi_n) + |C_{l+1}|^2 \sin[(l+1)\varphi_n]\} \exp\left(-\frac{r_0^2}{\rho^2}\sin^2\frac{\varphi_n}{2}\right)}{2\omega\rho^2(|C_l|^2 M_l + |C_{l+1}|^2 M_{l+1})}. \tag{48}$$

Since from Eqs. (44) and (45) one obtains $\frac{P_\perp}{W} = Q_l$, then using Eq. (47) it is possible to find out the specific intrinsic OAM M_{cz}. The results of numerical calculations are given in Fig. 11.

There is yet one more interesting feature concerned with the behavior of OAM of mode superposition. It relates to the transverse components of OAM. From Eq. (42) through Eqs. (14) and (34) one can easily obtain the expressions for transverse OAM:

$$\frac{M_x}{W} = \frac{n}{c}\bar{y}, \quad \frac{M_y}{W} = -\frac{n}{c}\bar{x}, \tag{49}$$

where for weakly guiding fibers $n_{co} \approx n_{cl} = n$ and c is the speed of light. Since also $P_z = \frac{n}{c}W$ one can derive from Eqs. (49) a simple connection:

$$\vec{M}_\perp = \vec{R}_c \times \vec{P}_\parallel, \tag{50}$$

where the symbol $\parallel$ specifies the longitudinal component of a vector. The last result enables one to determine a physical reason for the appearance of the lateral component of the OAM. The global longitudinal momentum is applied at the center of gravity C. If this point is shifted from the center O, the longitudinal momentum applied in C gives rise to the transverse AM. Such "mechanical" action of light has been established since Lebedev's experiments on demonstration of light pressure. This part of AM should be distinguished form the one that comes from the orbital motion of energy. Nevertheless it takes equal part in forming the total AM $\vec{M}$ and leads to the appearance of such interesting phenomenon as precession of OAM. For example, for the superposition of two DV modes taken with equal weights allowing for Eqs. (36) one readily obtains:

$$\frac{M_x}{W} = -\mathrm{R}_c \frac{n}{c}\sin[(\beta_{l+1} - \beta_l)z],$$

$$\frac{M_y}{W} = -\mathrm{R}_c \frac{n}{c}\cos[(\beta_{l+1} - \beta_l)z]. \tag{51}$$

Since M_z along with $M_\perp$ is conserved the vector $\vec{M}$ precesses about the z-axis as z increases (see Fig. 12). It should be emphasized that conservation of $M_\perp$, along with M_z and $|\vec{M}|$, takes place only for combination of two DVs with $\Delta l = 1$.

V. CONCLUSION

In the present paper, we have studied the field generated in the space by superposition of modes of a regular circular monomode fiber array. We proved that a supermode generates a discrete optical vortex, whose charge depends on the order of the supermode and the number of fibers in the array. We have studied the orbital angular momentum carried by a supermode and shown that it can be arbitrary low for well-spaced fibers. We proved that the angular momentum of superposition of modes equals the weighted sum of partial angular momenta. For certain combinations of supermodes the angular momentum comprises along with its intrinsic part also the extrinsic constituent. For such combinations precession of the angular momentum about the propagation axis takes place. We have also shown that by combining supermodes one can generate in the array stable regularly rotating field patterns, which should be identified with linear azimuthons. We have shown that by creating a phased excitation of certain groups of the array's fibers one can control the global motion of the excited domain thus achieving power switching between the fibers.

[1] J. F. Nye and M. V. Berry, Proc. R. Soc. London, Ser. A **336**, 165 (1974).

[2] J. F. Nye, *Natural Focusing and Fine Structure of Light: Caustics and Wave Dislocations* (Institute of Physics Publishing, Bristol, 1999).

[3] G. Indebetouw, J. Mod. Opt. **40**, 73 (1993); *Horizons of World Physics*, edited by M. Vasnetsov and K. Staliunas, (Nova Science, Huntington, N.Y., 1999), Vol. 228.

[4] M. S. Soskin, V. N. Gorshkov, M. V. Vasnetsov, J. T. Malos, and N. R. Heckenberg, Phys. Rev. A **56**, 4064 (1997).

[5] M. V. Berry, J. Opt. A, Pure Appl. Opt. **6**, 475 (2004); I. Freund, M. S. Soskin, and A. I. Mokhun, Opt. Commun. **208**, 223 (2002); F. Flossmann, K. O'Holleran, M. R. Dennis, and M. J. Padgettt, Phys. Rev. Lett. **100**, 203902 (2008).

[6] M. S. Soskin and M. V. Vasnetsov, Prog. Opt. **42**, 219 (2001).

[7] L. Allen, M. W. Beijersbergen, R. J. C. Spreeuw, and J. P. Woerdman, Phys. Rev. A **45**, 8185 (1992); L. Allen, M. J. Padgett, and M. Babiker, Prog. Opt. **39**, 291 (1999); L. Allen, S. M. Barnett, and M. J. Padgett, *Optical Angular Momentum* (Institute of Physics Publishing, Bristol, 2003); A. Bekshaev, M. Soskin, and M. Vasnetsov, *Paraxial Light Beams with Angular Momentum* (Nova Publishers, New York, 2008).

[8] T. Gahagan and G. A. Swartzlander, Jr., Opt. Lett. **21**, 827 (1996); H. He, M. E. J. Friese, N. R. Heckenberg, and H. Rubinsztein-Dunlop, Phys. Rev. Lett. **75**, 826 (1995); V. Garcés-Chávez, K. Volke-Sepulveda, S. Chávez-Cerda, W. Sibbett, and K. Dholakia, Phys. Rev. A **66**, 063402 (2002).

[9] G. S. Agarwal and J. Banerji, Opt. Lett. **27**, 800 (2002); G. Gibson *et al.*, Opt. Express **12**, 5448 (2004); Z. Bouchal and R. Chelechovsky, New J. Phys. **6**, 131 (2004).

[10] J. H. Lee, G. Foo, E. G. Johnson, and G. A. Swartzlander, Phys. Rev. Lett. **97**, 053901 (2006); G. A. Swartzlander, Jr. *et al.*, Opt. Express **16**, 10200 (2008).

[11] F. Tamburini, G. Anzolin, G. Umbriaco, A. Bianchini, and C. Barbieri, Phys. Rev. Lett. **97**, 163903 (2006); B. Spektor, A. Normatov, and J. Shamir, Appl. Opt. **47**, A78 (2008).

[12] M. E. J. Friese *et al.*, Appl. Phys. Lett. **78**, 547 (2001).

[13] A. Desyatnikov, Yu. Kivshar, and L. Torner, Prog, Opt. **47**, 291 (2005).

[14] A. Desyatnikov, C. Denz, and Yu. Kivshar, J. Opt. A, Pure Appl. Opt. **6**, S209 (2004); S. Lopez-Aguayo *et al.*, Opt. Lett. **31**, 1100 (2006).

[15] B. A. Malomed and P. G. Kevrekidis, Phys. Rev. E **64**, 026601 (2001); P. G. Kevrekidis, B. A. Malomed, and Yu. B. Gaididei, *ibid.* **66**, 016609 (2002).

[16] D. N. Neshev, T. J. Alexander, E. A. Ostrovskaya, Y. S. Kivshar, H. Martin, I. Makasyuk, and Z. Chen, Phys. Rev. Lett. **92**, 123903 (2004); J. W. Fleischer, G. Bartal, O. Cohen, O. Manela, M. Segev, J. Hudock, and D. N. Christodoulides, *ibid.* **92**, 123904 (2004).

[17] A. S. Desyatnikov and Yu. S. Kivshar, Phys. Rev. Lett. **88**, 053901 (2002).

[18] A. Ferrando, M. Zacares, and M.-A. Garcia-March, Phys. Rev. Lett. **95**, 043901 (2005).

[19] A. Ferrando, Phys. Rev. E **72**, 036612 (2005); M. A. García-March *et al.*, Physica D **238**, 1432 (2009).

[20] A. Ferrando, M. Zacares, M. A. Garcia-March, J. A. Monsoriu, and P. F. de Cordoba, Phys. Rev. Lett. **95**, 123901 (2005); A. Bezryadina *et al.*, Opt. Express **14**, 8317 (2006).

[21] A. Ferrando *et al.*, Opt. Express **12**, 817 (2004).

[22] B. Terhalle *et al.*, Phys. Rev. A **79**, 043821 (2009); T. J. Alexander, A. Desyatnikov, and Yu. Kivshar, Opt. Lett. **32**, 1293 (2007); K. J. H. Law, P. G. Kevrekidis, T. J. Alexander, W. Krolikowski, and Y. S. Kivshar, Phys. Rev. A **79**, 025801 (2009).

[23] F. Lederer *et al.*, Phys. Rep. **463**, 1 (2008); Y. V. Kartashov, V. A. Vysloukh, and L. Torner, Progr. Opt. **52**, 63 (2009); A. S. Desyatnikov, in *Discrete Vortices in Periodic Photonic Structures*, Fourth International Conference Singular Optics (Optical Vortices): Fundamentals and Applications SO'2008 (unpublished); A. A. Sukhorukov *et al.*, J. Opt. A, Pure Appl. Opt. **11**, 094016 (2009).

[24] T. J. Alexander, A. A. Sukhorukov, and Yu. S. Kivshar, Phys. Rev. Lett. **93**, 063901 (2004); E. A. Ostrovskaya and Yu. S. Kivshar, *ibid.* **93**, 160405 (2004).

[25] D. N. Christodoulides, F. Lederer, and Y. Silberberg, Nature (London) **424**, 817 (2003).

[26] A. Szameit, T. Pertsch, F. Dreisow, S. Nolte, A. Tunnermann, U. Peschel, and F. Lederer, Phys. Rev. A **75**, 053814 (2007); S. Longhi, Opt. Lett. **34**, 458 (2009); A. Szameit, I. L. Garanovich, M. Heinrich, A. A. Sukhorukov, F. Dreisow, T. Pertsch, S. Nolte, A. Tunnermann, and Y. S. Kivshar, Phys. Rev. Lett. **101**, 203902 (2008).

[27] H. B. Perets, Y. Lahini, F. Pozzi, M. Sorel, R. Morandotti, and Y. Silberberg, Phys. Rev. Lett. **100**, 170506 (2008).

[28] A. L. Jones, J. Opt. Soc. Am. **55**, 261 (1965).

[29] A. Yariv, *Quantum Electronics* (Wiley, New York, 1975).

[30] J. Hudgings, L. Molter, and M. Dutta, IEEE J. Quantum Elec-

tron. **36**, 1438 (2000).
[31] S. Longhi, J. Phys. B **40**, 4477 (2007).
[32] A. W. Snyder, J. Opt. Soc. Am. **62**, 1267 (1972); A. W. Snyder and J. D. Love, *Optical Waveguide Theory* (Chapman and Hall, London, New York, 1985).
[33] E. J. Bochove, Opt. Lett. **33**, 464 (2008).
[34] K. Hizanidis *et al.*, Phys. Scr. **T107**, 13 (2004).
[35] W. Królikowski *et al.*, Opt. Lett. **19**, 320 (1994).
[36] R. S. Kurti, K. Halterman, R. K. Shori, and M. J. Wardlaw, Opt. Express **17**, 13982 (2009).
[37] J. Wang and L. Wang, Appl. Opt. **48**, 881 (2009); V. H. Aristizabal, F. J. Velez, and P. Torres, Opt. Express **14**, 11848 (2006).
[38] R. Iwanow, D. A. May-Arrioja, D. N. Christodoulides, G. I. Stegeman, Y. Min, and W. Sohler, Phys. Rev. Lett. **95**, 053902 (2005).
[39] Ya. Izdebskaya, V. Shvedov, and A. Volyar, J. Opt. Soc. Am. A Opt. Image Sci. Vis **25**, 171 (2008); Ya. Izdebskaya *et al.*, Opt. Lett. **31**, 2523 (2006).
[40] Y. V. Kartashov, A. Ferrando, A. A. Egorov, and L. Torner, Phys. Rev. Lett. **95**, 123902 (2005).
[41] M. A. García-March, A. Ferrando, M. Zacarés, S. Sahu, and D. E. Ceballos-Herrera, Phys. Rev. A **79**, 053820 (2009).
[42] M. V. Berry, Proc. SPIE **3487**, 6 (1998).
[43] W. G. Bickley, *Bessel Functions and Formulae* (Cambridge University Press, Cambridge, 1953).
[44] C. N. Alexeyev, A. V. Volyar, and M. A. Yavorsky, in *Lasers, Optics and Electro-Optics Research Trends*, edited by L. I. Chen (Nova Publishers, New York, 2007), p. 131; C. N. Alexeyev *et al.*, J. Opt. A, Pure Appl. Opt. **10**, 055009 (2008).
[45] M. V. Berry, J. Opt. A, Pure Appl. Opt. **11**, 094001 (2009).
[46] N. Belabas *et al.*, Opt. Express **17**, 3148 (2009).
[47] V. V. Kotlyar, V. A. Soifer, and S. N. Khonina, Tech. Phys. Lett. **23**, 657 (1997); V. V. Kotlyar *et al.*, Opt. Commun. **274**, 8 (2007).
[48] A. S. Desyatnikov, A. A. Sukhorukov, and Yu. S. Kivshar, Phys. Rev. Lett. **95**, 203904 (2005); S. Lopez-Aguayo, A. Desyatnikov, and Yu. Kivshar, Opt. Express **14**, 7903 (2006).
[49] Z. Xu, Opt. Commun. **281**, 5605 (2008).
[50] A. Bekshaev and M. Soskin, Opt. Lett. **31**, 2199 (2006).
[51] A. Ya. Bekshaev, M. S. Soskin, and M. V. Vasnetsov, J. Opt. A, Pure Appl. Opt. **6**, S170 (2004); J. Opt. Soc. Am. A Opt. Image Sci. Vis **20**, 1635 (2003).
[52] R. Zambrini and S. M. Barnett, Phys. Rev. Lett. **96**, 113901 (2006).
[53] A. T. O'Neil, I. MacVicar, L. Allen, and M. J. Padgett, Phys. Rev. Lett. **88**, 053601 (2002).